

# Ship source level estimation and uncertainty quantification in shallow water via Bayesian marginalization

Dag Tollefsen, and Stan E. Dosso

Citation: [The Journal of the Acoustical Society of America](#) **147**, EL339 (2020); doi: 10.1121/10.0001096

View online: <https://doi.org/10.1121/10.0001096>

View Table of Contents: <https://asa.scitation.org/toc/jas/147/4>

Published by the [Acoustical Society of America](#)

---

## ARTICLES YOU MAY BE INTERESTED IN

[Estimation of seabed properties and range from vector acoustic observations of underwater ship noise](#)  
The Journal of the Acoustical Society of America **147**, EL345 (2020); <https://doi.org/10.1121/10.0001089>

[Source localization in the deep ocean using a convolutional neural network](#)  
The Journal of the Acoustical Society of America **147**, EL314 (2020); <https://doi.org/10.1121/10.0001020>

[Nonlinear time-warping made simple: A step-by-step tutorial on underwater acoustic modal separation with a single hydrophone](#)  
The Journal of the Acoustical Society of America **147**, 1897 (2020); <https://doi.org/10.1121/10.0000937>

[Seabed and range estimation of impulsive time series using a convolutional neural network](#)  
The Journal of the Acoustical Society of America **147**, EL403 (2020); <https://doi.org/10.1121/10.0001216>

[Machine learning in acoustics: Theory and applications](#)  
The Journal of the Acoustical Society of America **146**, 3590 (2019); <https://doi.org/10.1121/1.5133944>

[Deep ocean long range underwater navigation](#)  
The Journal of the Acoustical Society of America **147**, 2365 (2020); <https://doi.org/10.1121/10.0001081>

---



# Across Acoustics

The official podcast highlighting authors' research from our publications

# Ship source level estimation and uncertainty quantification in shallow water via Bayesian marginalization

.....  
**Dag Tollefsen<sup>1,a)</sup> and Stan E. Dosso<sup>2,b)</sup>**

<sup>1</sup>Norwegian Defence Research Establishment (FFI), Box 115, 3191, Horten, Norway

<sup>2</sup>School of Earth and Ocean Sciences, University of Victoria, Victoria, British Columbia V8W 3P6, Canada

*dag.tollefsen@ffi.no, sdosso@uvic.ca*

**Abstract:** This paper applies a non-linear Bayesian marginalization approach to ship spectral source level estimation in shallow water with unknown seabed properties and uncertain source depth. The algorithm integrates the posterior probability density over seabed models sampled via trans-dimensional Bayesian matched-field inversion and over depths/ranges of multiple point sources (representing different noise-generating components of a large ship) via Metropolis-Hastings sampling. Source levels and uncertainty are derived from marginal distributions for source strength. The approach is applied to radiated noise due to a container ship recorded on a bottom-moored horizontal array in shallow water. The average uncertainty is 3.8 dB/Hz for tonal frequencies. © 2020 Acoustical Society of America

[Editor: David R. Dowling]

Pages: EL339–EL344

**Received:** 31 January 2020 **Accepted:** 25 March 2020 **Published Online:** 17 April 2020

## 1. Introduction

This paper addresses the estimation of spectral source levels (SLs) and uncertainty in measurements on large container ships in shallow water, with *a priori* unknown seabed layering, seabed model parameters, and source depth. Measurements of the radiated noise level (RNL) of ships<sup>1,2</sup> has gained increasing interest in the assessment and monitoring of noise in marine environments. RNL measurements<sup>3</sup> typically require a deep-water site and defined test geometries to minimize environmental effects. For measurements on ships-of-opportunity (i.e., outside measurement ranges) and at shallow-water sites (where multipath and seabed interactions affect measurements), the specifications can be difficult to achieve. Alternatively, a monopole source level (MSL) definition has been adopted, using numerical propagation models to account for multipath and seabed effects. Recent work has addressed variability in MSL estimates in analysis of large data sets,<sup>4,6</sup> while the uncertainty in individual MSL estimates (addressed in this paper) has received little attention.

Probabilistic sampling over environment, source positions, and spectral levels (of multiple sources) has been employed in related work by Dosso and Wilmut<sup>7</sup> on Bayesian source localization, with source amplitude uncertainty and the coupling to environmental parameters quantified. Knobles<sup>8</sup> addressed ship SL estimation via a maximum-entropy inference method, with an application to shallow-water data with a half-space seabed model and a fixed-depth point source (to represent a small vessel) assumed.

The source model may also contribute to SL uncertainty. Gray and Greeley<sup>9</sup> used a fixed-depth point source to represent propeller-induced noise (the predominant source of ship-radiated noise). Wales and Heitmeyer<sup>4</sup> extended this to a Gaussian-distributed source depth model. The radiated noise of ships also comprises components due to other than the ship's propeller;<sup>10</sup> this seems not to have been incorporated in work on ship SL estimation.

## 2. Estimation algorithm

This section outlines the approach to SL estimation. Trans-dimensional Bayesian inference is used to address unknown seabed layering.<sup>11,12</sup> In this formulation, the posterior probability density (PPD) can be written

<sup>a)</sup>Author to whom correspondence should be addressed, ORCID: 0000-0002-2521-3817.

<sup>b)</sup>ORCID: 0000-0003-2384-7370.

$$P(k, \mathbf{m}_k | \mathbf{d}) = \frac{P(k)P(\mathbf{m}_k|k)P(\mathbf{d}|k, \mathbf{m}_k)}{\sum_{k' \in \mathcal{K}} \int_{\mathcal{M}_{k'}} P(k')P(\mathbf{m}'_k|k')P(\mathbf{d}|k', \mathbf{m}'_k) d\mathbf{m}'_k}, \tag{1}$$

where  $\mathcal{M}_k$  represents a  $M_k$ -dimensional space, indexed by  $k$ , specifying choices of model parameterization (number of seabed layer interfaces) with the corresponding sets of  $M_k$  free parameters denoted  $\mathbf{m}_k$ , and  $\mathbf{d}$  represents observed data. In Eq. (1),  $P(k)P(\mathbf{m}_k|k)$  is the prior probability of the state  $(k, \mathbf{m}_k)$ , and  $P(\mathbf{d}|k, \mathbf{m}_k)$  is the conditional probability of  $\mathbf{d}$  given  $(k, \mathbf{m}_k)$ , which is interpreted as the likelihood of  $(k, \mathbf{m}_k)$ , denoted  $L(k, \mathbf{m}_k)$ . The PPD is efficiently sampled using a reversible-jump Markov-chain Monte Carlo algorithm with principal-component reparameterization and parallel tempering.<sup>12</sup>

The data considered here consist of complex acoustic fields measured at an  $N$ -sensor array and  $F$  frequencies at  $S$  subsegments (snapshots) of the acoustic pressure time series, i.e.,  $\mathbf{d} = \{\mathbf{d}_{fs}, f=1, F; s=1, S\}$ .<sup>13</sup> The source spectrum is considered unknown over frequency and time with parameters  $A_{fs}$  and  $\theta_{fs}$  representing unknown amplitudes and phases, respectively. The data errors are assumed to be uncorrelated, circularly-symmetric complex Gaussian-distributed random variables, with unknown variances  $\nu_f$  which depend on frequency but are considered constant over snapshots and over hydrophones. The likelihood function for a single source is then given by

$$L(\mathbf{m}) = \prod_{f=1}^F \prod_{s=1}^S \frac{1}{(\pi\nu_f)^N} \exp \left[ -|\mathbf{d}_{fs} - A_{fs}e^{i\theta_{fs}}\mathbf{d}_f(\mathbf{m})|^2 / \nu_f \right], \tag{2}$$

where  $\mathbf{d}_f(\mathbf{m})$  represents replica data computed for model  $\mathbf{m}$  (the notation specifying the number of interfaces is omitted for simplicity). The explicit dependence on source spectral parameters and error variances can be removed by using maximum-likelihood (ML) estimates;<sup>7</sup> the ML-estimate for source amplitude is

$$\hat{A}_{fs} = \frac{|\mathbf{d}_f^H(\mathbf{m})\mathbf{d}_{fs}|}{|\mathbf{d}_f(\mathbf{m})|^2}. \tag{3}$$

Substituting the ML estimates back into Eq. (2) leads to the misfit (negative log-likelihood) function

$$E(\mathbf{m}) = N \sum_{f=1}^F \log_e \left\{ \text{Tr} \left[ \sum_{s=1}^S \mathbf{d}_{fs}\mathbf{d}_{fs}^H \right] - \frac{\sum_{s=1}^S |\mathbf{d}_{fs}^H\mathbf{d}_f(\mathbf{m})|^2}{|\mathbf{d}_f(\mathbf{m})|^2} \right\}. \tag{4}$$

Here,  $\text{Tr}\{\cdot\}$  and  $^H$  represent, respectively, the matrix trace and conjugate transpose. Explicitly sampling this misfit function over model parameters  $\mathbf{m}$  implicitly samples over the corresponding ML estimates for source spectrum and variances. Multiple point sources can be considered to represent different noise generating mechanisms on a ship. In this case each point source is assigned to correspond to a unique set of frequencies, and the misfit function Eq. (4) is summed over sources. Metropolis-Hastings sampling is applied to sample the position of each point source. Marginalization for a specific parameter (or pair of parameters) involves integrating the PPD over all other parameters to remove their effect from the resulting one-dimensional [or two-dimensional (2D)] marginal probability density. The marginal distribution for source amplitude  $A_f$  is given by marginalizing over environment, source positions, source phase, and noise variance,

$$P(A_f | \mathbf{d}) = \sum_{s=1}^S \int \delta(A_{fs} - \hat{A}_{fs}(\mathbf{m})) P(\mathbf{m} | \mathbf{d}_{fs}) d\mathbf{m}, \tag{5}$$

where  $\delta$  is the Dirac delta function. The SL and uncertainties follow from

$$\text{SL} = 20 \log_{10} \chi, \tag{6}$$

with  $\chi$  a statistical moment of the marginal distribution (i.e., computed from marginal distributions in linear units then converted to dB scale).

### 3. Results

The acoustic data considered were collected during the 2017 Seabed Characterization experiment on the New England Mud Patch,<sup>14</sup> with a 20-element horizontal line array (HLA) of length

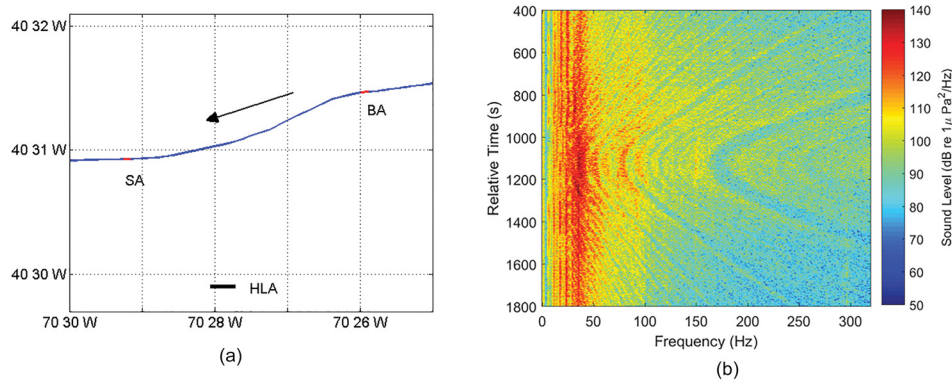


Fig. 1. (Color online) (a) Experiment area, container ship *M/V Ever Living* AIS track, location and orientation of the HLA, and approximate positions of data segments (BA and SA) analyzed. The arrow indicates the ship direction of travel. (b) Spectrogram of radiated noise due to the container ship.

480 m deployed in the north-eastern part of the experiment area [Fig. 1(a)]. Noise due to the container ship *M/V Ever Living* (length 335 m) approaching the HLA endfire direction from the east at range 4.12 km (bow aspect, angle  $319^\circ$ ) is considered first. The model environment consists of a water column with a measured sound speed profile over a layered seabed. The parameters that describe each homogeneous seabed layer are the interface depth ( $z_k$ ), sound speed ( $c_k$ ), density ( $\rho_k$ ), and attenuation coefficient ( $\alpha_k$ ). Prior bounds were set to 65–71 m for water depth, 1440–2100 m/s for sound speed, 1.2–2.4 g/cm<sup>3</sup> for density, and 0–0.5 dB/λ for attenuation in each seabed layer, with  $k = 1–3$  interfaces (maximum depth 60 m). Prior bounds on range  $r_{\text{AIS}} \pm 150$  m and depth  $[2, z_D]$  m were used for each source, with  $r_{\text{AIS}}$  the ship automatic identification system (AIS) position to array range, and  $z_D$  the maximum ship draft. Analysis of low-frequency tonals of the noise spectrogram [Fig. 1(b)] and knowledge of the ship’s parameters (Table 1) suggested a division of the frequency components included in the inversions (Table 2) into: (1) propeller-related tonals (B: 18–82 Hz), and (2) machinery-related tonals (F: 21–74 Hz). In addition, (3) a set of broadband (BB) components (BB: 180–290 Hz) were included. (See, e.g., Refs. 2 and 15 for analysis of ship spectra.) Inversions were run with three sources, one per set of frequency components. Data vectors were formed from time-series data sampled at 5 kHz, using Welch spectral estimation with 1-Hz fast Fourier transform resolution over  $S = 15$  consecutive, 50%-overlapping snapshots (each of duration 1 s).

Figure 2(a) shows marginal probability distributions for SL from Bayesian inversion, for three representative frequencies, one from each set F, B, and BB, in dB re  $1 \mu\text{Pa}^2 \text{m}^2/\text{Hz}$  (dB/Hz). (For display purposes, the histograms are here computed in dB units, with a bin width of 2 dB.) The distributions for B3 (18 Hz) and F3 (32 Hz) are unimodal, while at BB1 (180 Hz) there is also some probability in a secondary mode. Table 2 (left columns) shows the median SL estimates for the tonal frequencies, with uncertainties in terms of the inter-quartile range (IQR) interval. The highest SL is 188.0 dB/Hz at 32 Hz (tonal F3). The uncertainty interval is within 5.1–9.8 dB/Hz (dB-average 7.3 dB/Hz). The tonal SLs (162.3–188.0 dB/Hz) are overall lower than those reported in estimates on a container ship of comparable size at comparable speed [Fig. 7(b) of Ref. 2]: at 18–43 Hz by 3–6 dB/Hz, and at 64–82 Hz by 9–12 dB/Hz. The discrepancies may in

Table 1. Container ship parameters and characteristics.

Name	<i>M/V Ever Living</i>
IMO number	9 629 031
Gross tonnage	99 946
Maximum draft (m)	14.0
Length overall (m)	335
Breadth extreme (m)	45.8
Maximum capacity (TEU)	8508
Year built	2013
Number of cylinders	9
Number of propeller blades	5
Ship speed (knots)	18.0

Table 2. Frequency label (B—propeller-related and F—machinery-related tonals, the number indicates index in a harmonic series), frequency, median SL estimate, IQR uncertainty interval, from inversions of radiated noise from the container ship *M/V Ever Living*, at two aspects. (At 77–85 Hz, tonals included in the inversions differ between the data sets.) Source depth estimates (median with one-half IQR uncertainty) were for bow aspect B:  $4.8 \pm 0.8$  m, F:  $3.6 \pm 0.5$  m; for stern aspect B:  $7.5 \pm 2.5$  m, F:  $10.4 \pm 1.2$  m.

Frequency component	Frequency [Hz]	Bow aspect		Stern aspect	
		SL [dB/Hz]	IQR [dB/Hz]	SL [dB/Hz]	IQR [dB/Hz]
B3	18	185.8	6.7	194.1	6.9
B4	24	175.6	7.7	192.4	8.1
B5	29	178.6	9.8	190.4	7.5
B6	35	182.6	6.9	195.6	8.8
B13	77	164.5	6.9	—	—
B14	82	162.3	8.1	—	—
F2	21	187.1	8.6	181.2	7.0
F3	32	188.0	5.1	181.2	8.1
F4	43	178.3	8.1	179.6	7.1
F6	64	164.7	7.7	166.1	9.1
F7	74	163.0	7.9	168.8	6.6
F8	85	—	—	164.9	8.1

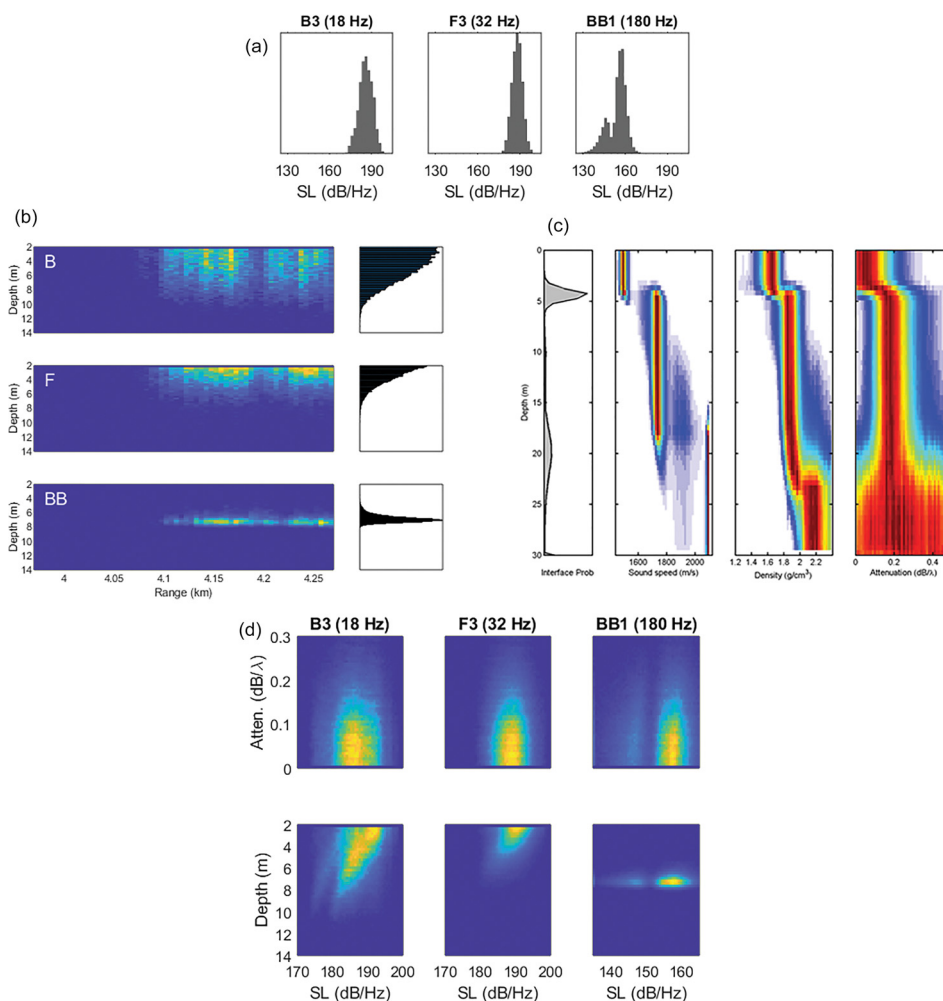


Fig. 2. (Color online) Results from Bayesian inversion of radiated noise due to the container ship *M/V Ever Living* at bow aspect. (a) Marginal probability distributions for SL at three frequencies (labels are B-propeller-related and F-machinery-related tonals, the number indicates index in a harmonic series, BB-broadband), (b) 2D source range/depth marginal probability distributions (left) and marginal probability distributions for source depth (right) for the three model sources, (c) marginal geoacoustic profiles, (d) 2D marginal probability distributions for SL/seabed attenuation (upper) and SL/source depth (lower) at three frequencies.

part be due to different aspect angles included in the measurements, and in part due to differences in the estimation procedures adopted.

Figure 2(b) shows 2D marginal probability distributions for source range/depth (left panels), and marginal probability distributions for source depth (right panels), for the three model sources. The distributions are elongated (and multimodal) in range, with median ranges (4.18–4.19 km) near the nominal range (4.12 km). Range uncertainty is in part due to the ship motion and in part due to an inherent range/water depth ambiguity in matched-field inversion. For sources B (propeller-related tonals) and F (machinery-related tonals), the depth is distributed over approximately 2–8 m, with a narrower distribution for source F than for source B. The median with one-half IQR uncertainty is  $4.8 \pm 0.8$  m and  $3.6 \pm 0.5$  m, respectively, for these two sources. For source BB (broadband noise), the depth is narrowly distributed at  $6.8 \pm 0.2$  m.

Figure 2(c) shows the estimated geoacoustic marginal profiles. These indicate a low-speed/low-density upper layer, a transition at 4–6 m depth, and a higher-speed/higher-density layer extending to approximately 20 m depth. The profiles are consistent with a layered mud-over-sand sediment model developed from previous ship-noise inversions in this area.<sup>13</sup> Geoacoustic and source position uncertainties contribute to SL uncertainty. To illustrate this, Fig. 2(d) (upper panels) shows 2D marginal distributions for SL/seabed attenuation (in the upper seabed) for three frequency components. The distributions indicate no correlation at the B3 and F3 frequencies, and weak positive correlation at BB1. Figure 2(d) (lower panels) shows 2D marginal distributions for SL/source depth. The distributions indicate strong negative correlation between source depth and SL at B3 (18 Hz, propeller noise) and F3 (32 Hz, machinery noise), but no correlation at the BB1 (180 Hz, BB noise) component. The correlation is likely related to the proximity to the pressure-release surface, i.e., the dipole effect.<sup>7</sup>

Figure 3(a) shows the SL estimates and uncertainties. The error bars indicate the upper and lower quartiles and the symbol is the median. The solid curve is the Wales-Heitmeyer reference spectrum<sup>4</sup> based on the mean of 54 merchant ship deep-water measurements. The dashed curve (Fig. 6 of Ref. 5, here adjusted for processing bandwidth) is the mean of a large ensemble of container ship measurements in shallow water. The SL estimates at 18–43 Hz are 5–20 dB higher than both reference curves. This may be expected since the estimates here are for prominent tonal frequencies for a specific ship, while the reference curves are based on averages over many ships whose tonals differ. Within uncertainty intervals, the SL estimates at 64–82 Hz encompass both reference curves; at 180–290 Hz the SL estimates encompass the Ref. 5 curve.

Table 2 (right columns) shows SL estimates (for tonal frequencies) from inversions of stern-aspect (angle 224°) data at range 2.75 km. The median SL is within 164.9–195.6 dB/Hz. The average uncertainty interval is 7.7 dB/Hz. Compared with bow-aspect data, the estimates are higher for all propeller-related frequencies (e.g., by 8.3 dB/Hz for B3, by 16.8 dB/Hz for B4), and lower for machinery-related frequencies: (e.g., by 5.9 dB/Hz for F2, by 6.8 dB/Hz for F3). This is consistent with other observations of different directionality for machinery- and propeller-related tonals.<sup>2,15</sup>

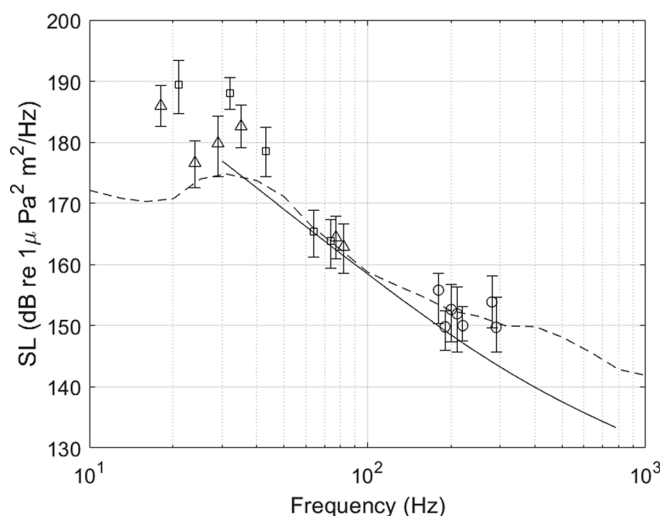


Fig. 3. Median SL estimates (symbols) with IQR uncertainty intervals (bars), from inversion of radiated noise due to the container ship *M/V Ever Living* at bow aspect. The curves are reference spectra from Ref. 4 (solid line), and from Ref. 5 (dashed line). (Symbols indicate: triangles—propeller-related tonals, squares—machinery-related tonals, circles—broadband noise).

#### 4. Summary

This paper developed and applied a Bayesian marginalization approach to ship spectral SL estimation with uncertain seabed layering, seabed geoacoustic properties, and uncertain depths/ranges of a number of model point sources (representing differing components of the radiated noise of a large ship). The algorithm samples the PPD over environmental parameters via trans-D sampling of a seabed of *a priori* unknown layering and over source depths/ranges via Metropolis-Hastings sampling. Marginal distributions for source strength were derived, with SL and uncertainties derived from the distributions. The approach was applied to radiated noise due to a container ship recorded on a bottom-moored HLA in the New England Mud Patch. The ship was modeled as three point sources, representing propeller-related tonals, machinery-related tonals, and broadband noise, respectively, with different posterior depth distributions obtained for each source. The average SL uncertainty of low-frequency tonals (in terms of one-half the IQR) was 3.8 dB/Hz. Within uncertainties, the SL estimates agreed well with reference spectra based on the mean of large ensembles of measurements on merchant ships.

#### Acknowledgments

Data from the New England Mud Patch (SBCEX) were collected with support from the ONR. The authors would like to thank the FFI engineering team and SBCEX chief scientists David P. Knobles and Preston S. Wilson.

#### References and links

- <sup>1</sup>M. F. McKenna, D. Ross, S. M. Wiggins, and J. A. Hildebrand, "Underwater radiated noise from modern commercial ships," *J. Acoust. Soc. Am.* **131**, 92–103 (2012).
- <sup>2</sup>M. Gassmann, S. M. Wiggins, and J. A. Hildebrand, "Deep-water measurements of container ship radiated noise signatures and directionality," *J. Acoust. Soc. Am.* **142**, 1563–1574 (2017).
- <sup>3</sup>ANSI/ASA, S12.64/Part 1, "American National Standard Quantities and Procedures for description and measurement of underwater sound from ships Part 1: General requirements" (American National Standards Institute and Acoustical Society of America, New York, 2009).
- <sup>4</sup>S. C. Wales and R. M. Heitmeyer, "An ensemble source spectra model for merchant-ship generated noise," *J. Acoust. Soc. Am.* **111**, 1211–1231 (2002).
- <sup>5</sup>A. O. MacGillivray, Z. Li, D. E. Hannay, K. B. Trounce, and O. M. Robinson, "Slowing deep-sea commercial vessels reduces underwater radiated noise," *J. Acoust. Soc. Am.* **146**, 340–351 (2019).
- <sup>6</sup>Y. Simard, N. Roy, C. Gervaise, and S. Giard, "Analysis and modeling of 255 source levels of merchant ships from an acoustic observatory along St. Lawrence Seaway," *J. Acoust. Soc. Am.* **140**, 2002–2018 (2016).
- <sup>7</sup>S. E. Dosso and M. J. Wilmut, "Bayesian multiple-source localization in an uncertain ocean environment," *J. Acoust. Soc. Am.* **129**, 3577–3589 (2011).
- <sup>8</sup>D. P. Knobles, "Maximum entropy inference on seabed attenuation parameters using ship radiated broadband noise," *J. Acoust. Soc. Am.* **138**, 3563–3575 (2015).
- <sup>9</sup>L. M. Gray and D. S. Greeley, "Source level model for propeller blade radiation for the world's merchant fleet," *J. Acoust. Soc. Am.* **67**, 516–522 (1980).
- <sup>10</sup>D. K. Wittekind, "A simple model for the underwater noise source level of ships," *J. Ship Prod. Des.* **30**, 1–8 (2014).
- <sup>11</sup>J. Dettmer and S. E. Dosso, "Trans-dimensional matched-field geoacoustic inversion with hierarchical error models and interacting Markov chains," *J. Acoust. Soc. Am.* **132**, 2239–2250 (2012).
- <sup>12</sup>S. E. Dosso, J. Dettmer, G. Steininger, and C. W. Holland, "Efficient trans-dimensional Bayesian inversion for geoacoustic profile estimation," *Inverse Prob.* **30**, 114018 (2014).
- <sup>13</sup>D. Tollefsen, S. E. Dosso, and D. P. Knobles, "Ship-of-opportunity noise inversions for geoacoustic profiles of a layered mud-sand seabed," *IEEE J. Oceanic Eng.* **45**, 189–200 (2020).
- <sup>14</sup>P. S. Wilson and D. P. Knobles, "An overview of the seabed characterization experiment," *IEEE J. Oceanic Eng.* **45**, 1–13 (2020).
- <sup>15</sup>P. T. Arveson and D. J. Vendittis, "Radiated noise characteristics of a modern cargo ship," *J. Acoust. Soc. Am.* **107**, 118–129 (2000).